Mistaking plastic for zooplankton: risk assessment of plastic ingestion in the Mediterranean sea

[Fabri-Ruiz, S[1,2]., Baudena, A[1]]*., Moullec F[3]., Lombard, F.[1], Irisson, J.-O[1]., Pedrotti, M.L[1].

[1]Sorbonne Université, CNRS, Laboratoire d'Océanographie de Villefranche, Villefranche-sur-Mer, France

[2] DECOD (Ecosystem Dynamics and Sustainability), IFREMER, INRAE, Institut Agro, Nantes, France

[3]Department of Coastal Systems, Royal Netherlands Institute for Sea Research, P.O. Box 59, 1790 AB Den Burg, Texel, The Netherlands

Corresponding authors: alberto.baudena@gmail.com, salome.fabri.ruiz@ifremer.fr

*co-first authors

Abstract

Floating plastic debris is a pervasive pollutant in seas and oceans, affecting a wide range of animals. In particular, microplastics (< 5 mm in size) increase the possibility that marine species consume plastic and enter the food chain. The present study investigates this potential mistake between plastic debris and zooplankton by calculating the plastic debris to zooplankton ratio over the whole Mediterranean Sea. To this aim, in situ data from the Tara Mediterranean Expedition are combined with environmental and Lagrangian diagnostics in a machine learning approach to produce spatially-explicit maps of plastic debris and

zooplankton abundance. We then analyse the plastic to zooplankton ratio in regions with high abundances of pelagic fish. Two of the major hotspots of pelagic fish, located in the Gulf of Gabès and Cilician basin, were associated with high ratio values. Finally, we compare the plastic to zooplankton ratio values in the Pelagos Sanctuary, an important hotspot for marine mammals, with other Geographical Sub-Areas, and find that they were among the larger of the Western Mediterranean Sea. Our results indicate a high potential risk of contamination of marine fauna by plastic and advocate for novel integrated modelling approaches which account for potential trophic transfer within the food chain.

I. Introduction

Plastic pollution is ubiquitous in the global ocean, from the sea surface to the seafloor (Woodall et al. 2014, Esposito et al., 2022), and represents a major threat to socio-economic services, tourism, and, ultimately, marine ecosystems (Aretoulaki et al., 2021; Beaumont et al., 2019). It is estimated that 19 to 23 million metric tons of plastic waste entered the aquatic systems in 2016, with an increasing trend expected in the next few years (Borrelle et al., 2020; Lau et al., 2020). The Mediterranean Sea is among the world's seas most polluted by plastic (Gerigny et al., 2019), with levels of concentration similar to those found in the Great Pacific Garbage Patch (Cózar et al., 2015; Pedrotti et al., 2022). At the same time, this quasi-enclosed sea is a key hotspot of marine biodiversity, with more than 17 000 species recorded (Coll et al., 2010), and supports an overall fishery activity of ca. 9 billion dollars every year (FAO 2020). Mediterranean marine ecosystems are, therefore, highly sensitive to plastic pollution (Solomando et al., 2022; Soto-Navarro et al., 2021). Understanding the magnitude of the impact of this pollutant on marine life is essential for conservation and

mitigation strategies (Galgani et al., 2014; Kershaw et al., 2019). In particular, it is fundamental to evaluate the risk of plastic transfer along marine trophic webs, including humans as well (Provencher et al., 2019; Rochman et al., 2015; Savoca et al., 2021). The need to assess microplastic risk at the scale of the Mediterranean sea is important considering the long distances crossed by mobile organisms (ie. cetaceans, fish, …). With the increase of multiple anthropogenic pressures (including microplastics) on these species, the risks must be evaluated at an appropriate spatial scale to mitigate their effect with adapted conservation measures. However, this understanding is hampered by the scarcity of available data, which usually cover only limited portions of the basin and differ in methodology (e.g., Mansui et al., 2020). In addition, only few studies measured plastic and organism concentrations concomitantly (Gérigny et al., 2022), making understanding of plastic impact difficult. In addition, the role of circulation on the distribution of plastic and zooplankton organisms is poorly unknown to date. An alternative method to estimate plastic concentration is the use of Lagrangian models. These are based on the release of virtual plastic particles which are then advected by current fields. From the virtual plastic trajectories different information can be obtained, including zones of potential accumulation or passage of plastic debris (Baudena et al., 2022, 2019; Beaumont et al., 2019; Liubartseva et al., 2019; Mansui et al., 2020) dispersion. Only a few have, however, been validated quantitatively with in situ data to date (Baudena et al., 2022). Furthermore, Lagrangian models only simulate plastic dispersion, and usually do not include biological activity such as the presence of zooplankton.

In the present study, we aim to quantify the relative presence of plastic compared to that of zooplankton, to assess the potential mistake encountered by marine predators. For this

purpose, we used in situ observations from the Tara Mediterranean Expedition, which constitutes the largest plastic dataset in the Mediterranean Sea to date: 122 stations covering the entire basin with homogenised and standardised sampling techniques. We considered plastic debris between 0.33—5.00 mm (usually referred to as *microplastics*). Microplastics constituted an important proportion of the plastic debris at sea, and were the vast bulk (~95%) of the debris collected during the Tara Mediterranean Expedition, making plastic estimates more reliable (Pedrotti et al., 2022). Importantly, along with plastic debris, zooplankton organisms of the same size class (0.33—5.00 mm) were concomitantly sampled. We then combined them with a machine learning approach to study the environmental drivers of plastic and zooplankton concentrations, unravelling some physical processes responsible for their distribution. With this information, we obtained spatial predictions for the whole Mediterranean Sea surface layer. These quantities were used to estimate a ratio between plastic debris and zooplankton abundance. This value represents the proportion of plastic debris with respect to the zooplankton organisms and can be seen as an indicator of potential impact on marine life. A ratio of 0.1 means that, for every ten zooplankton organisms present in a given seawater parcel, one plastic debris is present as well. Previous studies only estimated this metric in correspondence with the location of the sampling stations (Cole et al., 2011; Collignon et al., 2014; Doyle et al., 2011; Gérigny et al., 2022; Gove et al., 2019 (plastic:larval Fish) ; Lattin et al., 2004; Moore et al., 2002; Pedrotti et al., 2016). However, for conservation purposes, information on the impact of plastic at larger spatial scales is needed: here, we provide an estimate over the entire Mediterranean Sea of both plastic and zooplankton abundances as well as their ratio.

Furthermore, we use this metric to assess the overlap with potential predators through two

illustrative case studies. In the first, we only consider (i) species for which plastic ingestion has been reported (Fossi et al., 2014; Lefebvre et al., 2019; Pennino et al., 2020); (ii) species which are known to adopt non selective feeding strategies for certain prey sizes (Garrido et al., 2008, 2007; Queiros et al., 2019), as they could not be able to distinguish between plastic debris and zooplankton; (iii) species which are widely distributed over the entire Mediterranean basin (Bray et al., 2019); (iv) plastic debris and zooplankton in the same size class (0.33—5.00 mm) which can potentially confuse predators. As potential predators, we consider small pelagic fish (such as anchovies or sardines), which can acquire food through filter feeding behaviour. They feed on organisms smaller than 5 mm in size (Le Bourg et al., 2015) and have an important ecological and socio-economic role in the Mediterranean Sea. In the second case study, we focus on cetaceans by investigating the ratio values in the Pelagos sanctuary, which is a key foraging ground for marine mammals in the northwestern Mediterranean Sea (Croll et al., 2018; Fossi et al., 2014), and comparing them with Geographical Sub-Areas (GSAs) in the Mediterranean.

II. Materials and Methods

We used a machine learning approach to correlate the response (i.e., in situ plastic and zooplankton abundances data obtained from the Tara Mediterranean Expedition) and explanatory (i.e., physical and biogeochemical data and Lagrangian and Eulerian diagnostics) variables. In the following sections, we described the data and the modelling framework used as well as the methodology employed to determine the plastic to zooplankton ratio, which is then applied to two case studies. To ensure reproducibility and transparency of results, we provided an ODMAP (Overview, Data, Model, Assessment and Prediction)

protocol in the Supplementary Material. ODMAP is a standard protocol for species distribution models based-approach that we used in our study (Fitzpatrick et al., 2021; Zurell et al., 2020).

2.1. Response variables: in situ plastic and zooplankton data from Tara Mediterranean Expedition

The Tara Mediterranean Expedition was conducted in the Mediterranean Sea between June and November 2014. It sampled plastic debris and zooplankton in 122 stations across the whole basin (Figure 1), representing the largest coupled plastic zooplankton database in the Mediterranean Sea to date (Pedrotti et al., 2022). Plastic items were collected with a manta net (height 25 cm, width 60 cm, mesh size 333 µm) towed at the sea surface and at an average speed of ~2.5 knots for 60 minutes over a mean distance of ~4 km. Details of plastic processing are described in Pedrotti et al., (2022), and are briefly reported here. Plastic items were manually separated from zooplankton and organic tissue and scanned using the ZooScan system (Gorsky et al., 2010) under dry conditions, while zooplankton organisms were scanned separately under aqueous conditions. Particles and zooplankton were automatically detected and their morphological attributes were extracted by post-processing with Zooprocess and Plankton Identifier software. All obtained images were imported within EcoTaxa (http://ecotaxa.obs-vlfr.fr, Picheral et al., 2017) and classified in different taxonomic or particle categories. Microplastic (0.33—5 mm) abundances (in items per square km; N/km^2) were calculated from particle counts. In addition, plastic debris abundance was calculated also for the following size classes: debris between 0.33—1 mm; debris between 1—5 mm; all plastic debris collected (i.e., larger than 0.33 mm). The size

class limits were chosen in order to test the robustness of the results. Similarly, total zooplankton abundance per sample was calculated from zooscan and under the same size classes defined for plastic debris abundance. Diel vertical migration was not observed over the 24 hour day (Figure S1)

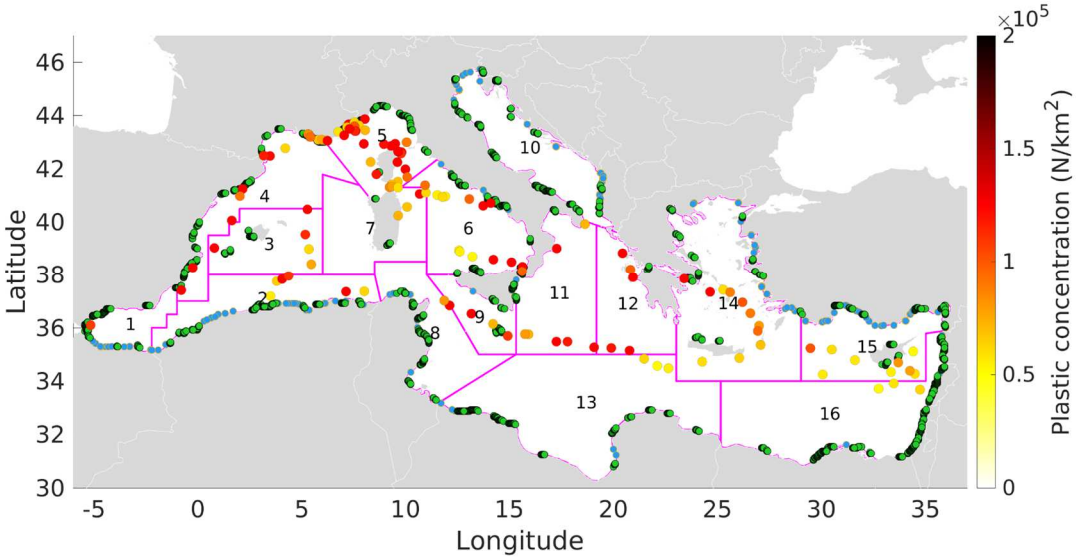

Figure 1 : Overview of the domain studied: Location of the 122 Tara Mediterranean Expedition stations (colored circles) and corresponding estimated plastic concentrations (right-hand yellow-to-red scale bar). Green and blue dots indicate the position of the coastal cities and river mouths used as potential plastic sources. The purple dashed lines separate the different Geographical Sub-Areas (GSAs) investigated in this study, indicated by a number. 1: Alboran Sea, 2: Algeria, 3: Balearic Islands, 4: Northern Spain and Gulf of Lion, 5: Pelagos sanctuary, 6: Tyrrhenian Sea, 7: Sardinia, 8: Tunisia, 9: Southern Sicily and Malta, 10: Adriatic Sea, 11: Western Ionian Sea, 12: Eastern Ionian Sea, 13: Southern Ionian Sea, 14: Aegean Sea, 15: Northern Levant Sea and Cyprus, 16 : Southern and Eastern Levant Sea

2.2. Explanatory variables

2.2.1. Physical and biogeochemical data : salinity, temperature, nitrates, phosphates, dissolved oxygen concentration

Physical and biogeochemical data were extracted from the Copernicus Marine Environment Monitoring Service (CMEMS, http://marine.copernicus.eu, product MEDSEA_REANALYSIS_PHYS_006_004) at 1/16° resolution. The product was supplied by the Nucleus for European Modelling of the Ocean (NEMO), with a variational data assimilation scheme (OceanVAR) for temperature and salinity vertical profiles and satellite Sea Level Anomaly along track data. We only considered the surface layer (Simoncelli et al., 2014). Physical and biogeochemical data were provided at daily and weekly resolution, respectively. Climatologies were calculated by averaging over the six months of the Tara Mediterranean Expedition (June to November 2014; Table S1). Spatial resolution was decreased from 1/16° to 1/8° by bilinear interpolation to fit the same spatial resolution of the Lagrangian and Eulerian diagnostics. The environmental explanatory variables obtained include mean values for temperature, salinity, phosphate, nitrate and dissolved oxygen concentration.

Zooplankton concentration (mass content of zooplankton expressed as carbon in seawater, g/km^2; Seapodym model; Lehodey et al., 2010) provided by the GLOBAL_MULTIYEAR_BGC_001_033 product (CMEMS platform) was used to calculate a zooplankton climatology between June and November 2014 at 0.083° spatial resolution. The latter was used as a qualitative reference for the zooplankton projection (Subsec. 4.1), and not as an explanatory variable.

2.2.2. Lagrangian and Eulerian diagnostics

Velocity field and trajectory calculation: The velocity field was obtained by combining

175 together two hydrodynamical fields, both downloaded from the CMEMS platform. The first
176 product was the MEDSEA_REANALYSIS_PHYS_006_004, which provides surface currents and
177 includes the geostrophic and the Ekman components. It has a spatial resolution of 1/16° and
178 a temporal resolution of one day. The second product was the
179 MEDSEA_HINDCAST_WAV_006_012. It provides drift due to waves (Stokes drift). It has a
180 spatial resolution of 1/24° and a temporal resolution of one day. The velocity fields were
181 spatially and temporally interpolated (bilinear interpolation) and summed together,
182 providing the final velocity field (1/24°; 1 hour). Thus, the surface currents used take into
183 account the Stokes drift, which indirectly includes windage, an important component for
184 microplastic transport in marine environments (Onink et al., 2019), especially in the
185 Mediterranean Sea (Liubartseva et al., 2018). As zooplankton samplings were collected at
186 the same depth as plastic debris, we used the same velocity field for both explanatory
187 variables. Trajectories were calculated with a 4^{th} order Runge-Kutta scheme in both space
188 and time, with a time step of 20 minutes.
189
190 **Lagrangian and Eulerian diagnostics description:** Different Lagrangian and Eulerian
191 diagnostics were used as explanatory variables. Lagrangian diagnostics were derived from
192 trajectories, whereas Eulerian diagnostics were obtained by properties at a fixed location.
193 The Eulerian diagnostics calculated were: *Absolute velocity*: $U=\mathrm{sqrt}(u^2+v^2)$, with *u* and *v*
194 being the zonal and meridional component of the velocity field; *Kinetic Energy* = u^2+v^2
195 which, together with the absolute velocity is considered as a proxy of the intensity of the
196 currents; *Vorticity*: denotes the presence (when positive or negative) or absence (when
197 close to 0) of eddies; *Okubo-Weiss*: When negative (positive), this metric indicates a water
198 parcel inside (outside) an eddy; *Turbulent Kinetic Energy (TKE)*: This metric analyses the

199 standard deviation of the velocity field time series and quantifies whether a region was
200 subjected to strong turbulence. The Lagrangian diagnostics calculated were: *Finite-Time*
201 *Lyapunov Exponents (FTLE)*: FTLEs quantify the rate of separation due to currents. They are
202 used to identify barriers to transport or regions affected by strong turbulence (Baudena et
203 al., 2021; d'Ovidio et al., 2004); *Lagrangian Betweenness*: this metric is used to identify
204 regions that act as "bottlenecks" for the circulation, i.e. in which water parcels of multiple
205 origins pass and then go to several different destinations (Ser-Giacomi et al., 2021);
206 *Retention time*: this metric estimates the amount of time a water parcel spent inside an
207 eddy (if it was inside it) (d'Ovidio et al., 2015); *Lagrangian divergence*: this metric calculates
208 the Eulerian divergence along the backward trajectory. When negative (positive), it indicates
209 convergence (divergence) of water masses, and can be used as a proxy of downwelling
210 (upwelling) Hernández-Carrasco et al., (2018); *Lagrangian Plastic Pollution Index (LPPI)*: this
211 metric estimates the amount of plastic debris in a water parcel based on the plastic sources
212 (cities and rivers, blue and green dots in Fig. 1) encountered along the water parcel's
213 previous path. The water parcel "encounters" a plastic source when it passes below a
214 distance threshold from it (details in Pedrotti et al., 2022).
215 As for the physical and biogeochemical explanatory variables, climatologies of Lagrangian
216 and Eulerian diagnostics were calculated between June and November 2014 at 1/8° of
217 spatial resolution over the entire Mediterranean Sea. Details about the different parameters
218 used for each of the diagnostics are reported in Supplementary Table S2.

219 **2.3. Modelling framework: Xgboost models**

220 **2.3.1. Collinearity between explanatory variables**

221 Multicollinearity occurs when two or more explanatory variables in a multiple regression

model are highly correlated, which means that one can be predicted linearly from the others with a high degree of accuracy. Multicollinearity can cause data redundancy in the explanatory variables which can lead to model overfitting or reduction in model predictive ability (Dormann et al., 2013). If multicollinearity patterns differ between fitted data in the model and new data, large errors could be introduced in the predictions. To restrict these possible biases, multicollinearity between explanatory variables was initially examined using variance inflation (VIF) factors in a stepwise procedure (Dormann et al., 2013). VIF is computed from equation [1], where R^2_j is obtained from a regression between variable j^{th} against all other explanatory variables.

$$VIF_j = \frac{1}{1-R_j^2} \quad [1]$$

In a stepwise procedure, the function calculates VIF values for all explanatory variables, removes the variable with the highest value, and repeats until all VIF variable values are below a given threshold (here 5). Finally, we computed Spearman pairwise correlation (r_S) between descriptors and removed one of the two descriptors when correlation values of r_S were above 0.7 (Dormann et al., 2013). Analyses were performed using the usdm (Babak, 2015) and corrplot (Wei et al., 2017) R packages. Table S3 lists the remaining variables used in Xgboost models for each category.

2.3.2. Parameterization and calibration of XGboost models

The extreme gradient boosting (XGBoost) modelling approach (Chen and Guestrin, 2016) was used to model plastic debris and zooplankton abundances for each size class. Xgboost is an efficient gradient machine learning method that combines two algorithms: first, simple

245 and small regression trees, calculated on random subsets of data while minimising residuals;
246 and subsequently boosting, which combines all the models into a unique solution (for
247 statistical details see Chen and Guestrin, 2016). XGBoost models are able to fit complex
248 functions, which could reflect the complexity of processes shaping plastic debris and
249 zooplankton patterns. Xgboost models were performed using the xgboost R package (Chen
250 et al., 2015).
251 Cross validation procedure was used to estimate the best parameters of the xgboost model.
252 This procedure uses a single parameter k that refers to the number of groups for a given
253 dataset to be split into. In our case, we used k=4. For each group, we take the remaining
254 groups as a training data set and use the selected group to evaluate the model. This
255 procedure was performed for different xgboost parameters and poisson distribution:
256 number of trees (1 to 900), maximum depth (2, 4, 6) where the higher is the value the more
257 complex the model is, eta (0.005, 0.01, 0.02, 0.03, 0.04) which is the learning rate,
258 min_child_weigth (1, 5) which defines the minimum sum of weights of all observations
259 required in a child (used to control over-fitting). Best parameters were selected by
260 minimising the negative log-likelihood for Poisson regression. We evaluated the model using
261 the R^2 coefficient between observed and predicted data. Because several distance threshold
262 values were provided for plastic data (based on the LPPI), we fitted models for each and
263 kept the best one (Table S4).

264 **2.3.3. Prediction and projection**

265 The partial dependence plots (PDP) technique (Friedman, 2001) was used to achieve a
266 graphical representation of the marginal effect of a variable on the response variable. We
267 also extract variable importance from the model, which shows how a feature is important in

making a branch of a decision tree purer. A high percentage means important explanatory variables which constrain response variables. Calculated functions in the model were then used to extrapolate plastic debris and zooplankton abundances for each grid cell over the entire Mediterranean Sea at a period corresponding to June-November 2014. We projected mean plastic debris and zooplankton abundances and associated standard deviations.

2.4. Plastic to zooplankton ratio definition

Using zooplankton and plastic debris abundance projections over the entire Mediterranean Sea, we calculated the plastic debris to zooplankton ratio (amount of plastic debris divided by the amount of zooplankton) at 1/8° of spatial resolution. For each grid cell *i*, the ratio was obtained by dividing the plastic and the zooplankton abundances (expressed in N/km^2) of the same size class *j*:

$$Ratio_{i,j} = \frac{Plastic\ abundance_{i,j}}{Zooplankton\ abundance_{i,j}} \quad (1)$$

Equation 1 implies that, for example, if the ratio equals 0.1, for every 1000 zooplankton organisms in a given water parcel 100 plastic debris of similar size is present. The ratio was calculated using plastic debris and zooplankton organisms of size classes between 0.33—5 mm. Ratios calculated using different size classes (Subsec. 2.1) are reported in Supplementary Materials. The uncertainty on the ratio was calculated with the variance formula using the plastic and zooplankton associated standard deviations and Equation (1). The ratio obtained using the size class of 0.33—5 mm was evaluated (i) in the Pelagos Sanctuary, a hotspot for cetaceans, representing a foraging ground for different whale species (Morgado et al., 2017). The ratio in the Pelagos Sanctuary was compared with the

ratio calculated in the Mediterranean GSAs (Fig. 1). GSAs were obtained from the FAO platform (https://www.fao.org/gfcm/data/maps/gsas/en/). In order to have GSAs of similar surface area, we merged together the following GSAs: Northern Alboran Sea, Southern Alboran Sea, and Alboran Island, creating the Alboran Sea GSA (GSA 1); Northern Spain and Gulf of Lion GSA (GSA 4); Ligurian Sea and Northern Tyrrhenian Sea and Southern and Central Tyrrhenian Sea, creating the Tyrrhenian Sea GSA (GSA 6); Western and Eastern Sardinia, creating the Sardinia GSA (GSA 7); Northern Tunisia, Gulf of Hammamet, and Gulf of Gabès, creating the Tunisia GSA (GSA 8); Southern Sicily and Malta GSA (GSA 9); Northern and Southern Adriatic Sea, creating the Adriatic Sea GSA (GSA 10); Crete and Aegean Sea, creating the Aegean Sea GSA (GSA 14); Northern Levant Sea and Cyprus, creating the Northern Levant Sea and Cyprus GSA (GSA 15); Southern and Eastern Levant Sea GSA (GSA 16). In addition, the Corsica GSA was not considered because it was included in the Pelagos Sanctuary, while the Gulf of Lion and Ligurian Sea and Northern Tyrrhenian Sea were reduced to avoid overlap with the Pelagos Sanctuary.

The ratio values in the Pelagos Sanctuary and in the GSAs were compared using a paired sample Wilcoxon test with corrections applied for multiple testing; (ii) in the Mediterranean areas where the total biomass of small pelagic fish is large according to simulations provided by the end-to-end ecosystem model OSMOSE-MED (Moullec et al., 2019b). Results for the other size classes are available in the Supplementary Material.

2.5. The end-to-end model OSMOSE-MED

OSMOSE-MED is an end-to-end modelling chain, including a general circulation model, a regional climate model, a regional biogeochemistry model and a multispecies dynamic

315 model (OSMOSE; Moullec et al., 2019). OSMOSE is a spatially explicit individual-based model
316 which simulates the whole life cycle of several interacting fish and macro-invertebrates
317 species from eggs to adult stages. Major ecological processes of the life cycle, such as
318 growth, predation, reproduction, and mortality sources, are modelled step by step (15 days
319 in this study) (www.osmose-model.org; (Shin et al., 2004; Shin and Cury, 2001). OSMOSE-
320 MED covers the whole Mediterranean Sea and represents the Mediterranean food web
321 from pankton to main top-predators in the 2006-2013 period. Hundred marine species (fish,
322 cephalopods and crustaceans), representing ca. 95% of total declared catches in the region
323 over the 2006-2013 period were explicitly modelled. For a full description of the
324 parameterization and calibration of OSMOSE-MED (see Moullec et al., 2022, 2019a, 2019b).
325 The biomass of small pelagic fish is an output of OSMOSE-MED simulations. As OSMOSE is a
326 stochastic model, ten replicated simulations were run and averaged to analyse the outputs.
327 For this study, the total biomass of 10 small pelagic species only (e.g., European anchovy,
328 European sardine, Round sardinella or European sprat) was considered. Areas of small-
329 pelagic high biomass were defined as the locations with a biomass value higher than the
330 90th percentile of all the Mediterranean Sea biomass values. Results corresponding to the
331 80th and 95th percentiles are reported in the Supplementary Materials.
332

333 ## III. Results

334 ### 3.1. Plastic and zooplankton distributions in the Mediterranean Sea and their drivers

335 The predictive performance of the Xgboost model was assessed by calculating the
336 correlation coefficient (R^2) between observed and predicted values of plastic and
337 zooplankton abundance (Table 1, S4, S5, Figure S2, S3). R^2 coefficients were 0.68 and 0.57

for plastic debris and zooplankton abundances, respectively (Table 1). Overall, the relationships found tended to overestimate low values and to underestimate large ones (Figure S2, S3). R^2 is known to be sensitive to the extent of dependent variables (Gelman and Hill, 2006) which range between 2260 N/km² and 7974561 N/km² in this study. This could explain the low cross-validated R^2 which is strengthened by the low amount of available data (122 sampling stations). High zooplankton abundances were associated with negative Okubo-Weiss values (19 % of the explanatory power in the model, Fig. 2c), and with positive and negative vorticity values (14%). Both these explanatory variables indicate an eddy presence, and do not reveal a clear preference for cyclones or anticyclones. The temperature influenced the total zooplankton abundance as well (16%), with lower abundances associated with higher temperatures. Attracting fronts, identified by Finite-Time Lyapunov Exponents (FTLEs, 9%) calculated backward in time, were positively correlated with zooplankton abundance, while the relationship was of opposite sign with diverging fronts (FTLE forward in time: 8%; and divergence: 7%). Explanatory variables that most contributed to explain plastic debris abundance were the kinetic energy (50%) and TKE (10%) (Figure 2d), indicating a greater concentration of plastic debris in retentive and low turbulence regions. Nitrates (11%, a proxy for riverine outputs) indicated a positive relationship between plastic debris presence and the proximity to river mouths.

When considering the plastic and zooplankton abundances projected over the entire Mediterranean Sea (Fig. 2a,b), highest concentrations were mainly observed in the Adriatic and Aegean Seas (GSAs 10 and 14 in Fig. 1, respectively). In these regions, abundances were estimated around 20×10^6 N/km^2 for zooplankton (Figure 2a) and 5×10^6 N/km^2 for plastic debris (Figure 2b). The Eastern basin (GSAs 15 and 16) presented low abundances of

zooplankton and plastic debris. However, the latter was abundant along Cyprus (located in GSA 15) and Lebanon (located in GSA 16) coasts and in the Gulf of Gabès (located in GSA 8). The Tyrrhenian Sea (GSA 6) was also a hotspot of plastic debris abundance. In the Strait of Gibraltar (located in GSA 1), the models predicted high values of zooplankton abundances and low plastic debris concentrations.

The results obtained with different size classes showed very similar patterns (Figure S4, S5 and S6), and high R^2 coefficients were obtained as well (Table S5). Plastic standard deviation maps (Fig. S7a) show that the uncertainties corresponded to about 10% of the plastic abundance values. The same considerations were valid for the zooplankton uncertainties (Fig. S7b), showing the robustness of the models obtained.

Table 1 : Predictive performance and best parameters estimated by 4-fold cross validation for size between 0.33 and 5 mm

	Predictive performance	**Model parameters**			
Group	**R^2**	**trees**	**Maximum depth**	**Eta**	**Minimum child weight**
Zooplankton (> 0.33 and < 5 mm)	0.57	707	2	0.04	5
Microplastic (> 0.33 and < 5 mm)	0.68	851	2	0.03	1

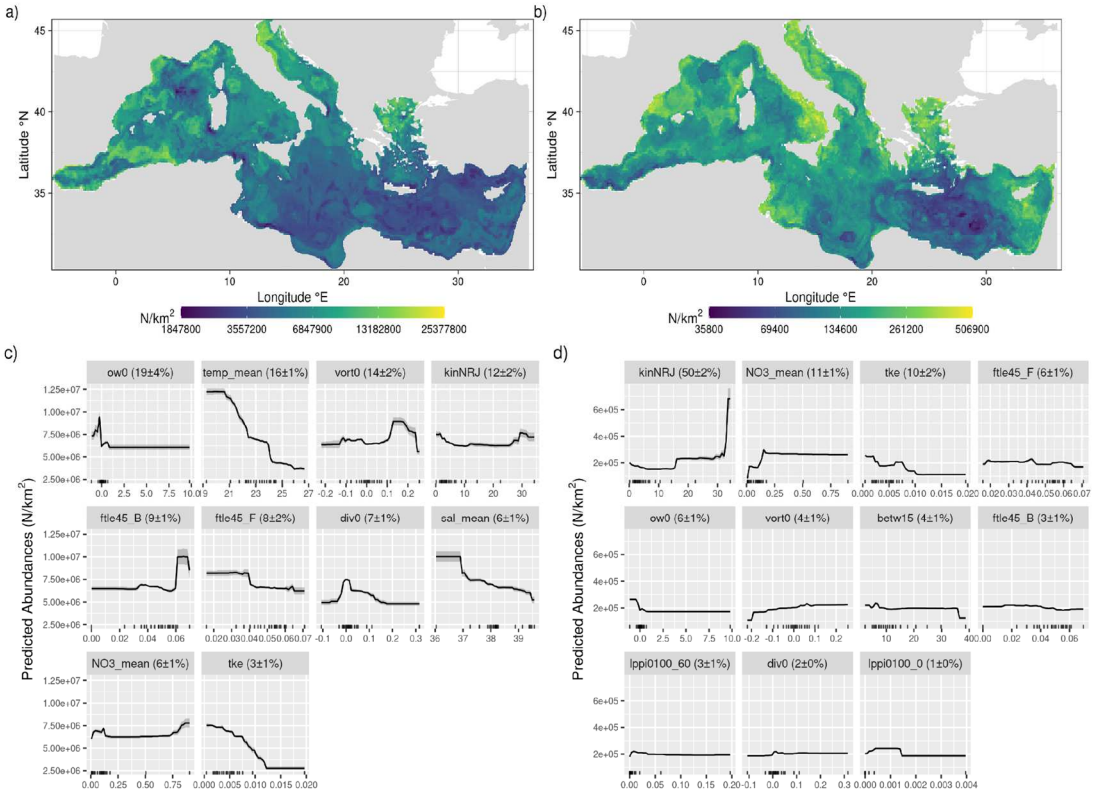

375

376 **<u>Figure 2</u> : Plastic and zooplankton abundances :** Spatial projection and partial dependence
377 plot of zooplankton (panels a and c, respectively) and plastic debris abundance (panels b
378 and d, respectively) for the size class < 5 mm. oW0 = Okubo Weiss, kinNRJ = Kinetic Energy,
379 temp_mean = mean temperature, NO3_mean = mean nitrate concentration, vort0 =
380 vorticity , tke = Turbulent Kinetic Energy, ftle45_F = FTLE 45 days forward in time, ftle45_B =
381 FTLE 45 days backward in time, div0 = Eulerian Divergence, betw15 = Betweenness at 15
382 days, sal_mean = mean salinity, lppi0100_60 = LPPI with distance threshold of 1° and 60
383 days backward in time, lppi0100_0 = LPPI with distance threshold of 1° and no advection

384 **3.2. Plastic to zooplankton ratio**

385 Using zooplankton and plastic debris abundance projections, we calculated the plastic to
386 zooplankton ratio (number of plastic debris per km^2 divided by the number of zooplankton

387 organisms per km^2 , MM 2.4) over the entire Mediterranean Sea for the size class between
388 0.33—5 mm (Fig. 3a). The average plastic to zooplankton ratio was 0.029 (±0.012) at the
389 Mediterranean scale. Areas with the highest average plastic to zooplankton ratio were the
390 gulf of Gabès (located in GSA 8), the Cilician (GSA 15), the Levantine (GSA 15 and 16), and
391 the Southern Tyrrhenian Seas (GSA 6), with values of ~0.10. Intermediate values (~0.05)
392 were found in the Balearic (GSA 3) and Adriatic Seas (GSA 3) and in the Central
393 Mediterranean (GSA 13). Lower values (~ 0.01) were in the Alboran Sea (GSA 1) and the
394 central sector of the Eastern Mediterranean Sea (GSA 16 and eastern part of GSA 15).

395 When considering the results obtained with different size classes the spatial pattern did not
396 change consistently (Fig. S10). The ratio decreased to 0.004—0.1 when considering a size
397 class between 0.33—1 mm, while it increased to 0.005—0.3 when considering the size class
398 between 1 and 5 mm, due to the different abundances considered. The uncertainty on the
399 ratio (Fig. S7c) was greater in regions of larger ratio and lower elsewhere, and corresponded
400 to ~10% of the ratio value. These results show the soundness of this metric.

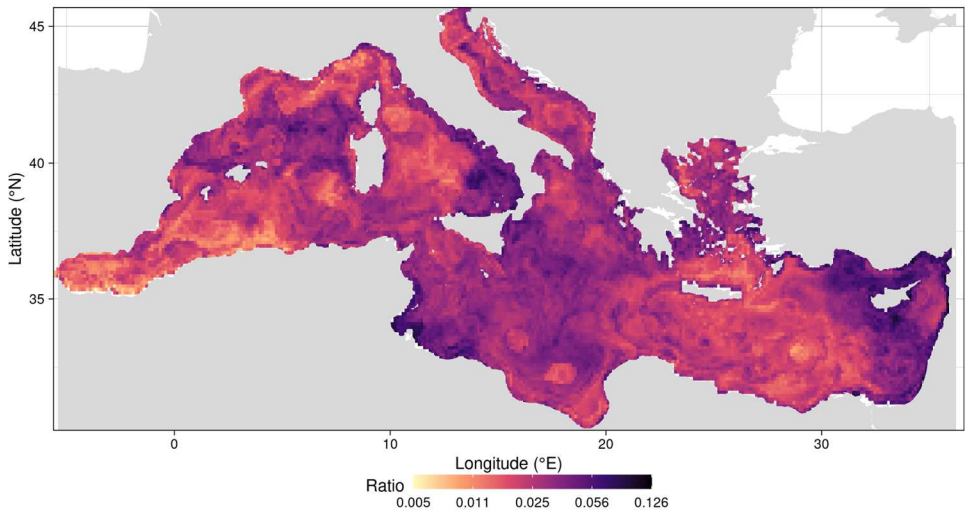

401

402 **Figure 3 : Plastic to zooplankton ratio** : Spatial projection of the plastic to zooplankton ratio

403 for the size class between 0.33—5 mm

404 **3.3. Case studies**

405

406 **3.3.1. Wildlife exposure: plastic ingestion risk for small pelagic fish**

407

408 The plastic to zooplankton ratio was applied to two case studies to analyse the probability of

409 plastic ingestion by wildlife as described in the next subsections.

410 In the first case study, we considered the total biomass of small pelagic fish in the

411 Mediterranean Sea for the time period 2006-2013, obtained from the Osmose model.

412 One of the largest Mediterranean hotspots of small pelagic fish, located in the Gulf of Gabès

413 (located in GSA 8), as well as a smaller one in the Cilician basin (between Cyprus and Turkey,

414 GSA 15), were found in correspondence with plastic to zooplankton ratios greater than 0.06

(Fig. 4a). Two large hotspots of small pelagic fish, in the Adriatic Sea (GSA 10) and in the Southern Catalan Sea (GSA 4), were associated with moderate plastic to zooplankton ratios greater than 0.03. The remaining part of the small pelagic hotspots was highly patchy and mainly distributed along the coasts, with variable ratio values.

When using different percentiles to identify the main small pelagic fish hotspots (Fig. S9), these were still located in the Adriatic Sea and in the Gulf of Gabès, confirming that these hotspots were threatened by plastic pollution and providing evidence of the robustness of the analyses.

3.3.2 Wildlife exposure: plastic ingestion risk in the Pelagos Sanctuary and different Mediterranean regions

In the second case study, we calculated the plastic to zooplankton ratio in the Pelagos Sanctuary and compared it with the ratio of 15 Mediterranean Sea GSAs (Fig.1). The Pelagos Sanctuary showed ratio values which were significantly larger than those predicted in the Alboran Sea (GSA 1), Algeria (GSA 2), Balearic Islands (GSA 3), Northern Spain and Gulf of Lion (GSA 4) and Aegean Sea (GSA 14), while they were significantly lower than those in the Tyrrhenian Sea (GSA 6), Southern Sicily and Malta (GSA 9), and the Northern Levant Sea (GSA 16). No significant differences were found with other GSAs (Fig. 4b).

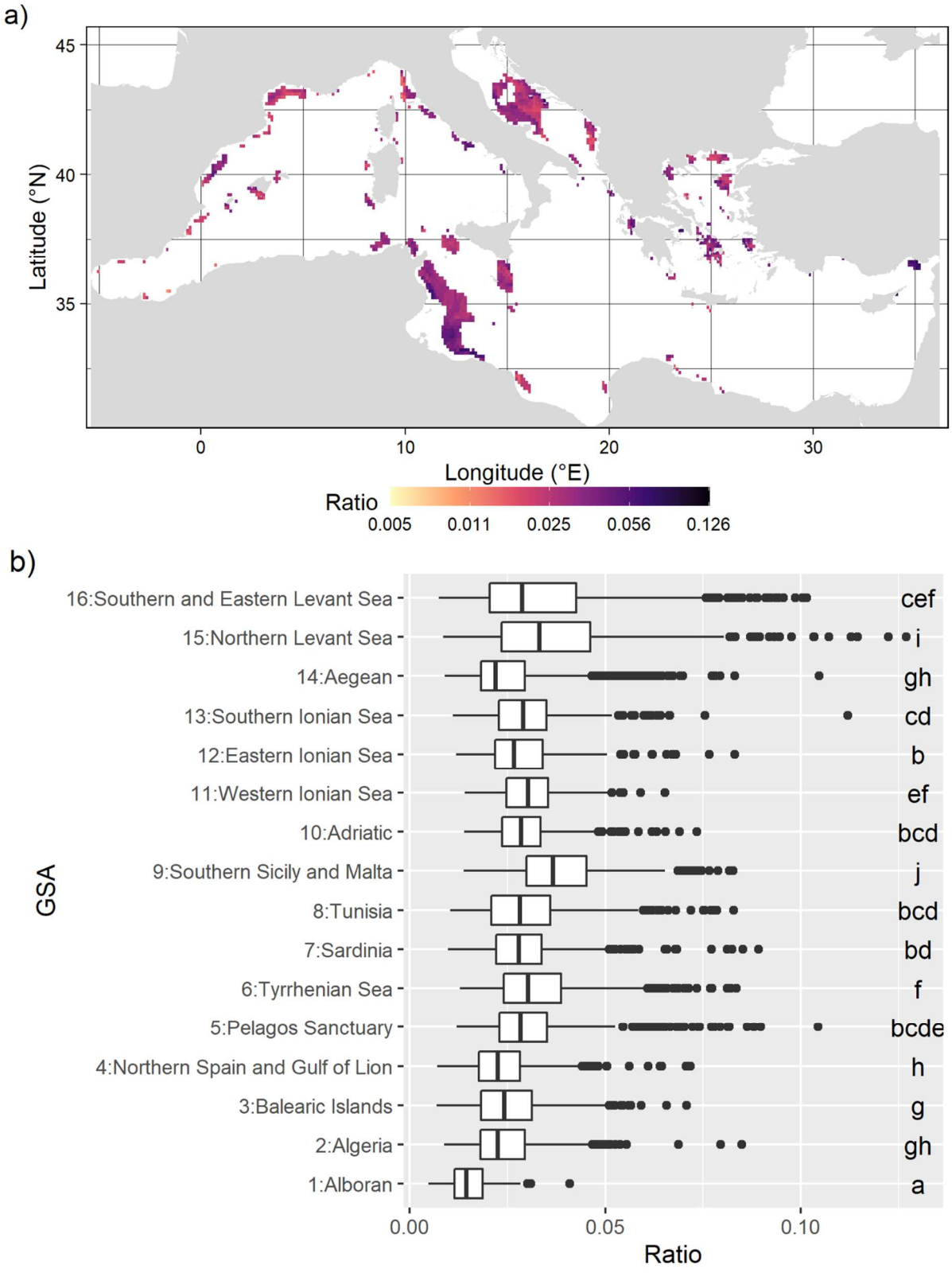

436

437 **Figure 4 : Application of plastic to zooplankton ratio to two case studies :**a) Plastic to

438 zooplankton ratio for plastic debris of size between 0.33—5 mm, showed only in

439 correspondence with the hotspots of small pelagic fish (defined as the locations with a
440 biomass larger than the 90th percentile), b) boxplot of ratio values in the Pelagos Sanctuary
441 and in 15 Mediterranean GSAs (shown in Fig. 1, MM 4). The letters on top of each box
442 display pairwise wilcoxon test results.

443

444 ## IV. Discussion

445 ### 4.1. Zooplankton distribution in the Mediterranean Sea and its drivers

446

447 Zooplankton abundance was boosted by eddy presence, even if no clear preference for
448 cyclones or anticyclones was detected. This was in accordance with previous studies finding
449 large zooplankton concentration in eddies (Chambault et al., 2019; Godø et al., 2012;
450 Riandey et al., 2005). Temperature played an important role in zooplankton abundances
451 which decreased when temperature increased. This is because temperature affects the
452 mixed layer depth (MLD) (D'Ortenzio et al., 2005). MLD governs the availability of nutrients
453 and light, which are essential for phytoplankton, the primary food source for zooplankton.
454 In regions with higher temperatures, such as the Levantine Basin, the MLD is relatively
455 shallow (due to a low mixing in winter and a strong stratification in summer): this hampers
456 nutrient supply to the phytoplankton, and in turn inhibits zooplankton growth; conversely,
457 in the western basin, colder, the MLD is deeper, boosting biological activity (D'Ortenzio et
458 al., 2005). High zooplankton abundance in coastal regions can also be attributed to
459 phytoplankton blooms occurring near highly populated coasts, subject to terrigenous and
460 river inputs in nutrients (Siokou-Frangou et al., 2010).
461 Frontal converging regions (identified through backward FTLE) were positively correlated

462 with zooplankton abundance. This is in coherence with previous studies highlighting the
463 importance of these features for mid trophic levels and, in general, the whole trophic chain
464 (Baudena et al., 2021; Chambault et al., 2017; d'Ovidio et al., 2010; Della Penna et al., 2015).
465 The negative correlation found with diverging zones (identified through forward FTLE and
466 divergence) suggest that these structures, even if fostering primary production, hamper
467 zooplankton concentration, possibly by spreading it away.
468 Notably, the pattern of zooplankton abundance over the whole Mediterranean was in
469 agreement with the average zooplankton mass in June–November 2014 obtained by the
470 Seapodym model (Lehodey et al., 2010; Fig. S11): the western Mediterranean showed larger
471 values than the eastern Mediterranean; the largest values were predicted in the northern
472 Adriatic Sea and in the Algerian and Alboran basins both by our projection and by the
473 Seapodym model. Differences could be explained by the fact that we used zooplankton
474 abundance (in N/km^2) while Seapodym provided zooplankton mass, and by the different
475 methodological approaches.
476
477 **4.2. Plastic debris distribution in the Mediterranean Sea and its drivers**
478
479 Plastic debris concentration obtained from the projections was lower in regions
480 characterised by strong currents and turbulence. This was confirmed by the decreasing
481 relationship found between plastic debris and kinetic energy (50 % of the variance), TKE,
482 and FTLE calculated both forward and backward in time (Fig. 2d). The positive relationship
483 found with nitrates, a proxy for land-based pollution (e.g. river mouths or cities), indicated
484 that plastic debris abundance was linked with coastal sources. This suggests that plastic
485 debris is released mainly from coastal sources, in coherence with previous studies (Baudena

et al., 2022; Liubartseva et al., 2018), where less energetic features are found. When plastic debris moves offshore, turbulent activity and currents mix it, lowering plastic abundance. This is corroborated by the slightly negative relationship with FTLE calculated both forward and backward in time: plastic debris may be attracted by frontal converging regions but then spread away.

The projection of plastic concentration does not show regions of strong plastic accumulation. This is in coherence with previous studies (Baudena et al., 2022; Liubartseva et al., 2018), which attributed this lack to the strong spatio-temporal variability of Mediterranean currents.

The plastic concentration pattern we obtained was similar to the one reported by (Liubartseva et al., 2018) despite the different methodological approach (a Lagrangian tracking model). Higher concentrations of plastic debris were found in the northern Adriatic and (GSA 10) in the Balearic and northern Spain Sea (GSAs 3 and 4) and in the Levantine Basin (GSAs 15 and 16). Lower concentrations were found in the central part of the Eastern Mediterranean (GSAs 14—16), in the Bomba Gulf (Southern part of GSA 13), and in the Alboran Sea (GSA 1). A larger concentration was predicted in the Cilician basin (GSA 15) and in a portion of the Gulf of Lion (GSA 4) by Liubartseva et al. (2018) model, likely driven by the nearby presence of coastal plastic sources. This result provides evidence of the soundness of the pattern we obtained.

Our model predicted a total of $4 \cdot 10^{11}$ plastic debris floating at the surface of the Mediterranean Sea. This value was in agreement with the results from (Pedrotti et al., 2022); $6 \cdot 10^{11}$, confidence interval 4—$14 \cdot 10^{11}$). The difference may be explained by the fact that our model predicted the plastic debris concentration over the entire basin and not only at the location of the Tara Mediterranean Expedition stations.

In general, plastic models had better estimations than zooplankton models. This may be due to the relatively easier description of plastic dynamics rather than zooplankton abundance, which is driven by complex biological and ecological processes including growth, predation, competition or behaviour including vertical migrations (Queré et al., 2005).

4.3. Plastic to zooplankton ratio and wildlife exposure

The plastic and zooplankton projections allowed us to calculate the plastic to zooplankton ratio at the Mediterranean Sea scale. This ratio ranged approximately between 0.005 (i.e., 5 plastic debris every 1000 zooplankton organisms) and 0.100 (i.e., 100 plastic debris every 1000 zooplankton organisms) throughout the whole basin.

Our results on the risk of plastic ingestion for small pelagic fish suggested that they could ingest large amounts of debris. Indeed, the ratio of plastic to zooplankton was moderate to high in the two larger pelagic fish hotspots, located in the Gulf of Gabès (GSA 8) and in the Adriatic Sea (GSA 10). This is of particular concern since both regions are heavily exploited by fishing industries (Colloca et al., 2017). While we could not explicitly observe an ingestion of plastic debris by small pelagic fish in situ, previous studies reported microplastic presence in the stomach content of at least 87 fish species in the Mediterranean Sea (Habib et al., 2021), many of them being commercially important (Jâms et al., 2020; Renzi et al., 2019).

The Pelagos Sanctuary showed plastic to zooplankton ratio values (0.031±0.014) significantly larger than all the GSAs in the Western Mediterranean, with the exclusion of the Tyrrhenian Sea, and which were comparable to several GSAs across the basin. This value was similar to the average plastic to zooplankton ratio obtained in the northwestern Mediterranean by Pedrotti et al., (2016) (2016; 0.03 ±1.40). These results highlight the potential ingestion of

534 plastic debris by whales in this region. Fossi et al., (2012) recorded phthalates (a main
535 constituent of plastic) in fin whale *Balaenoptera physalus* blubber, showing that they could
536 consume plastic debris directly or indirectly from water and plankton. Hence, these
537 mammals, among the largest filter feeders in the world and adapted to absorbing large
538 quantities of prey in a single mouthful, are threatened in one of their main feeding areas
539 which is heavily contaminated.
540 We stress that the latter cases are just two examples of how the plastic to zooplankton ratio
541 can be used to estimate the threat represented by plastic debris on marine biota and,
542 ultimately, on human health (Bhuyan et al., 2022). Several other applications are possible,
543 including the study of marine protected areas (Soto-Navarro et al., 2021), fishery grounds
544 (Colloca et al., 2017), or specific regional analyses, also unravelling the origin of the plastic
545 debris (Liubartseva et al., 2019).
546
547 **4.4. Limits**
548
549 The present study is not a mechanistic understanding of plastic debris ingestion by small
550 pelagic fish. Zooplankton communities and their quality as food supply for predators were
551 not assessed. Feuilloley et al. (2022), using a long time series of zooplankton observations in
552 the northwestern Mediterranean, showed that changes in zooplankton composition, size,
553 and density may impact higher trophic levels, such as the fitness of small pelagic fish.
554 Results should be considered cautiously as both plastic and zooplankton were averaged over
555 6 months in the same year (June—November 2014). We only analysed surface data, while
556 zooplankton organisms live in the whole water column and several species have a diel
557 vertical migration.

558 It was not possible to identify a value of plastic to zooplankton ratio over which the risk of
559 plastic ingestion could be considered high, as no studies have investigated this question to
560 date. A possible choice would be the percentile of the ratio distribution over the
561 Mediterranean Sea. However, as the plastic pollution is expected to increase in the future
562 (Borrelle et al., 2020; Lau et al., 2020), so will the ratio. Further studies are needed on this
563 issue.
564 Multiple caveats are associated with the use of statistical approaches in a dynamic
565 environment: i) they did not allow us to establish a causal relationship between
566 plastic/zooplankton abundances and environment; ii) they have limited capacities to
567 extrapolate in space and time (Guisan and Thuiller, 2005; Ralston and Moore, 2020; Yates et
568 al., 2018). However, these approaches have proved to be useful, valuable, and cost-effective
569 tools to quantify plastic/zooplankton distribution, especially in data-poor areas (Fabri-Ruiz
570 et al., 2019; Guillaumot et al., 2019).
571
572
573
574 **V. Conclusions**
575
576 All in all, our findings showed that plastic debris is widespread in the Mediterranean Sea,
577 with a number of debris in a similar order of magnitude than zooplankton organisms across
578 the entire basin. This highlights the potential stress induced by this invasive element on the
579 marine ecosystems, and the necessity of further research efforts on these questions.
580 Further samplings of plastic debris and zooplankton organisms are needed, with larger
581 spatio-temporal resolutions and water column observations. In addition, the understanding

582 of the interaction between top predators, fish, and lower trophic levels in the presence of
583 plastic will be crucial to correctly assess the threat encountered and to design mitigation
584 strategies.

585

586 **Acknowledgments and funding**

587

588 We thank the commitment of the following institutions: CNRS, Sorbonne University, LOV.
589 The Tara Ocean Foundation and its founders and sponsors: agnès b.®, Etienne Bourgois, the
590 Veolia Environment Foundation, Lorient Agglomeration, Serge Ferrari, the Foundation
591 Prince Albert II of Monaco, IDEC, the "Tara" schooner, crews and teams. We thank
592 MERCATOR-CORIOLIS and ACRI-ST for providing daily satellite data during the expedition.
593 We are also grateful to the French Ministry of Foreign Affairs for supporting the expedition
594 and to the countries that graciously granted sampling permission. The authors are grateful
595 to Enrico Ser-Giacomi for his helpful advice on the design of the research. This study was
596 financed by the French Ministry for Ecological Transition (MTES) who supported a post-
597 doctoral fellowship for Salome Fabri-Ruiz and EU H2020 LABPLAS project under the grant
598 agreement (ID: 101003954), DOI: 10.3030/101003954.

599

600 **Data availability**

601

602 All the data necessary to produce the figures of the Main Text, i.e. the plastic and
603 zooplankton abundances calculated over the whole Mediterranean Sea, the plastic to
604 zooplankton ratio, the partition of the different GSAs used, as well as the climatology of the

small pelagic fish biomass are available at https://doi.org/10.5281/zenodo.7076175. The in situ plastic concentrations are available at https://doi.org/ 10.5281/zenodo.5538237. The velocity field used to calculate the Lagrangian diagnostics are available on the E.U. Copernicus Marine Environment Service Information website (CMEMS, http://marine.copernicus.eu/).

References

Aretoulaki, E., Ponis, S., National Technical University Athens, Plakas, G., National Technical University Athens, Agalianos, K., National Technical University Athens, 2021. Marine plastic littering: a review of socio economic impacts. J. Sustain. Sci. Manag. 16, 276–300. https://doi.org/10.46754/jssm.2021.04.019

Babak, N., 2015. usdm: Uncertainty analysis for species distribution models. R package version 1.1-15.

Baudena, A., Ser-Giacomi, E., D'Onofrio, D., Capet, X., Cotté, C., Cherel, Y., D'Ovidio, F., 2021. Fine-scale structures as spots of increased fish concentration in the open ocean. Sci. Rep. 11, 15805. https://doi.org/10.1038/s41598-021-94368-1

Baudena, A., Ser-Giacomi, E., Jalón-Rojas, I., Galgani, F., Pedrotti, M.L., 2022. The streaming of plastic in the Mediterranean Sea. Nat. Commun. 13, 2981. https://doi.org/10.1038/s41467-022-30572-5

Baudena, A., Ser-Giacomi, E., López, C., Hernández-García, E., d'Ovidio, F., 2019. Crossroads of the mesoscale circulation. J. Mar. Syst. 192, 1–14. https://doi.org/10.1016/j.jmarsys.2018.12.005

Beaumont, N.J., Aanesen, M., Austen, M.C., Börger, T., Clark, J.R., Cole, M., Hooper, T., Lindeque, P.K., Pascoe, C., Wyles, K.J., 2019. Global ecological, social and economic impacts of marine plastic. Mar. Pollut. Bull. 142, 189–195. https://doi.org/10.1016/j.marpolbul.2019.03.022

Bhuyan, Md.S., Rashed-Un-Nabi, Md., Alam, Md.W., Islam, Md.N., Cáceres-Farias, L., Bat, L., Musthafa, M.S., Senapathi, V., Chung, S.Y., Núñez, A.A., 2022. Environmental and Morphological Detrimental Effects of Microplastics on Marine Organisms to Human Health (preprint). In Review. https://doi.org/10.21203/rs.3.rs-1290795/v1

Borrelle, S.B., Ringma, J., Law, K.L., Monnahan, C.C., Lebreton, L., McGivern, A., Murphy, E., Jambeck, J., Leonard, G.H., Hilleary, M.A., Eriksen, M., Possingham, H.P., De

Frond, H., Gerber, L.R., Polidoro, B., Tahir, A., Bernard, M., Mallos, N., Barnes, M., Rochman, C.M., 2020. Predicted growth in plastic waste exceeds efforts to mitigate plastic pollution. Science 369, 1515–1518. https://doi.org/10.1126/science.aba3656

Bray, L., Digka, N., Tsangaris, C., Camedda, A., Gambaiani, D., de Lucia, G.A., Matiddi, M., Miaud, C., Palazzo, L., Pérez-del-Olmo, A., Raga, J.A., Silvestri, C., Kaberi, H., 2019. Determining suitable fish to monitor plastic ingestion trends in the Mediterranean Sea. Environ. Pollut. 247, 1071–1077. https://doi.org/10.1016/j.envpol.2019.01.100

Chambault, P., Baudena, A., Bjorndal, K.A., Santos, M.A.R., Bolten, A.B., Vandeperre, F., 2019. Swirling in the ocean: Immature loggerhead turtles seasonally target old anticyclonic eddies at the fringe of the North Atlantic gyre. Prog. Oceanogr. 175, 345–358. https://doi.org/10.1016/j.pocean.2019.05.005

Chambault, P., Roquet, F., Benhamou, S., Baudena, A., Pauthenet, E., de Thoisy, B., Bonola, M., Dos Reis, V., Crasson, R., Brucker, M., Le Maho, Y., Chevallier, D., 2017. The Gulf Stream frontal system: A key oceanographic feature in the habitat selection of the leatherback turtle? Deep Sea Res. Part Oceanogr. Res. Pap. 123, 35–47. https://doi.org/10.1016/j.dsr.2017.03.003

Chen, T., Guestrin, C., 2016. XGBoost: A Scalable Tree Boosting System, in: Proceedings of the 22nd ACM SIGKDD International Conference on Knowledge Discovery and Data Mining. Presented at the KDD '16: The 22nd ACM SIGKDD International Conference on Knowledge Discovery and Data Mining, ACM, San Francisco California USA, pp. 785–794. https://doi.org/10.1145/2939672.2939785

Chen, T., He, T., Benesty, M., Khotilovich, V., Tang, Y., Cho, H., Chen, K., 2015. Xgboost: extreme gradient boosting. R Package Version 04-2 1, 1–4.

Cole, M., Lindeque, P., Halsband, C., Galloway, T.S., 2011. Microplastics as contaminants in the marine environment: A review. Mar. Pollut. Bull. 62, 2588–2597. https://doi.org/10.1016/j.marpolbul.2011.09.025

Coll, M., Piroddi, C., Steenbeek, J., Kaschner, K., Ben Rais Lasram, F., Aguzzi, J., Ballesteros, E., Bianchi, C.N., Corbera, J., Dailianis, T., Danovaro, R., Estrada, M.,

685 Froglia, C., Galil, B.S., Gasol, J.M., Gertwagen, R., Gil, J., Guilhaumon, F., Kesner-
686 Reyes, K., Kitsos, M.-S., Koukouras, A., Lampadariou, N., Laxamana, E., López-Fé
687 de la Cuadra, C.M., Lotze, H.K., Martin, D., Mouillot, D., Oro, D., Raicevich, S., Rius-
688 Barile, J., Saiz-Salinas, J.I., San Vicente, C., Somot, S., Templado, J., Turon, X.,
689 Vafidis, D., Villanueva, R., Voultsiadou, E., 2010. The Biodiversity of the
690 Mediterranean Sea: Estimates, Patterns, and Threats. PLoS ONE 5, e11842.
691 https://doi.org/10.1371/journal.pone.0011842
692 Collignon, A., Hecq, J.-H., Galgani, F., Collard, F., Goffart, A., 2014. Annual variation in
693 neustonic micro- and meso-plastic particles and zooplankton in the Bay of Calvi
694 (Mediterranean–Corsica). Mar. Pollut. Bull. 79, 293–298.
695 https://doi.org/10.1016/j.marpolbul.2013.11.023
696 Colloca, F., Scarcella, G., Libralato, S., 2017. Recent Trends and Impacts of Fisheries
697 Exploitation on Mediterranean Stocks and Ecosystems. Front. Mar. Sci. 4, 244.
698 https://doi.org/10.3389/fmars.2017.00244
699 Cózar, A., Sanz-Martín, M., Martí, E., González-Gordillo, J.I., Ubeda, B., Gálvez, J.Á.,
700 Irigoien, X., Duarte, C.M., 2015. Plastic Accumulation in the Mediterranean Sea.
701 PLOS ONE 10, e0121762. https://doi.org/10.1371/journal.pone.0121762
702 Croll, D.A., Tershy, B.R., Newton, K.M., de Vos, A., Hazen, E., Goldbogen, J.A., 2018. Filter
703 feeding, in: Encyclopedia of Marine Mammals. Elsevier, pp. 363–368.
704 d'Ovidio, F., De Monte, S., Alvain, S., Dandonneau, Y., Lévy, M., 2010. Fluid dynamical
705 niches of phytoplankton types. Proc. Natl. Acad. Sci. 107, 18366–18370.
706 https://doi.org/10.1073/pnas.1004620107
707 d'Ovidio, F., Della Penna, A., Trull, T.W., Nencioli, F., Pujol, M.-I., Rio, M.-H., Park, Y.-H.,
708 Cotté, C., Zhou, M., Blain, S., 2015. The biogeochemical structuring role of horizontal
709 stirring: Lagrangian perspectives on iron delivery downstream of the Kerguelen
710 Plateau. Biogeosciences 12, 5567–5581. https://doi.org/10.5194/bg-12-5567-2015
711 d'Ovidio, F., Fernández, V., Hernández-García, E., López, C., 2004. Mixing structures in the
712 Mediterranean Sea from finite-size Lyapunov exponents: Mixing structures in the

713 Mediterranean sea. Geophys. Res. Lett. 31, n/a-n/a.
714 https://doi.org/10.1029/2004GL020328
715 Della Penna, A., De Monte, S., Kestenare, E., Guinet, C., d'Ovidio, F., 2015. Quasi-
716 planktonic behavior of foraging top marine predators. Sci. Rep. 5, 18063.
717 https://doi.org/10.1038/srep18063
718 Dormann, C.F., Elith, J., Bacher, S., Buchmann, C., Carl, G., Carré, G., Marquéz, J.R.G.,
719 Gruber, B., Lafourcade, B., Leitão, P.J., Münkemüller, T., McClean, C., Osborne,
720 P.E., Reineking, B., Schröder, B., Skidmore, A.K., Zurell, D., Lautenbach, S., 2013.
721 Collinearity: a review of methods to deal with it and a simulation study evaluating
722 their performance. Ecography 36, 27–46. https://doi.org/10.1111/j.1600-
723 0587.2012.07348.x
724 D'Ortenzio, F., Iudicone, D., de Boyer Montegut, C., Testor, P., Antoine, D., Marullo, S.,
725 Santoleri, R., Madec, G., 2005. Seasonal variability of the mixed layer depth in the
726 Mediterranean Sea as derived from in situ profiles: mixed layer depth over the
727 Mediterranean. Geophys. Res. Lett. 32, n/a-n/a.
728 https://doi.org/10.1029/2005GL022463
729 Doyle, M.J., Watson, W., Bowlin, N.M., Sheavly, S.B., 2011. Plastic particles in coastal
730 pelagic ecosystems of the North-East Pacific ocean. Mar. Environ. Res. 71, 41–52.
731 https://doi.org/10.1016/j.marenvres.2010.10.001
732 Fabri□Ruiz, S., Danis, B., David, B., Saucède, T., 2019. Can we generate robust species
733 distribution models at the scale of the Southern Ocean? Divers. Distrib. 25, 21–37.
734 https://doi.org/10.1111/ddi.12835
735 Feuilloley, G., Fromentin, J.-M., Saraux, C., Irisson, J.-O., Jalabert, L., Stemmann, L., 2022.
736 Temporal fluctuations in zooplankton size, abundance, and taxonomic composition
737 since 1995 in the North Western Mediterranean Sea. ICES J. Mar. Sci. 79, 882–900.
738 https://doi.org/10.1093/icesjms/fsab190
739 Fitzpatrick, M.C., Lachmuth, S., Haydt, N.T., 2021. The ODMAP protocol: a new tool for
740 standardized reporting that could revolutionize species distribution modeling.

741 Ecography 44, 1067–1070. https://doi.org/10.1111/ecog.05700
742 Fossi, M.C., Coppola, D., Baini, M., Giannetti, M., Guerranti, C., Marsili, L., Panti, C., de
743 Sabata, E., Clò, S., 2014. Large filter feeding marine organisms as indicators of
744 microplastic in the pelagic environment: The case studies of the Mediterranean
745 basking shark (*Cetorhinus maximus*) and fin whale (*Balaenoptera physalus*). Mar.
746 Environ. Res. 100, 17–24. https://doi.org/10.1016/j.marenvres.2014.02.002
747 Fossi, M.C., Panti, C., Guerranti, C., Coppola, D., Giannetti, M., Marsili, L., Minutoli, R.,
748 2012. Are baleen whales exposed to the threat of microplastics? A case study of the
749 Mediterranean fin whale (*Balaenoptera physalus*). Mar. Pollut. Bull. 64, 2374–2379.
750 https://doi.org/10.1016/j.marpolbul.2012.08.013
751 Friedman, J.H., 2001. Greedy function approximation: a gradient boosting machine. Ann.
752 Stat. 1189–1232.
753 Galgani, F., Claro, F., Depledge, M., Fossi, C., 2014. Monitoring the impact of litter in large
754 vertebrates in the Mediterranean Sea within the European Marine Strategy
755 Framework Directive (MSFD): Constraints, specificities and recommendations. Mar.
756 Environ. Res. 100, 3–9. https://doi.org/10.1016/j.marenvres.2014.02.003
757 Garrido, S., Ben-Hamadou, R., Oliveira, P., Cunha, M., Chícharo, M., van der Lingen, C.,
758 2008. Diet and feeding intensity of sardine *Sardina pilchardus*: correlation with
759 satellite-derived chlorophyll data. Mar. Ecol. Prog. Ser. 354, 245–256.
760 https://doi.org/10.3354/meps07201
761 Garrido, S., Marçalo, A., Zwolinski, J., van der Lingen, C., 2007. Laboratory investigations on
762 the effect of prey size and concentration on the feeding behaviour of *Sardina*
763 *pilchardus*. Mar. Ecol. Prog. Ser. 330, 189–199. https://doi.org/10.3354/meps330189
764 Gelman, A., Hill, J., 2006. Data Analysis Using Regression and Multilevel/Hierarchical
765 Models. Cambridge University Press.
766 Gerigny, O., Brun, M., Fabri, M.C., Tomasino, C., Le Moigne, M., Jadaud, A., Galgani, F.,
767 2019. Seafloor litter from the continental shelf and canyons in French Mediterranean
768 Water: Distribution, typologies and trends. Mar. Pollut. Bull. 146, 653–666.

https://doi.org/10.1016/j.marpolbul.2019.07.030

Gérigny, O., Pedrotti, M.-L., El Rakwe, M., Brun, M., Pavec, M., Henry, M., Mazeas, F., Maury, J., Garreau, P., Galgani, F., 2022. Characterization of floating microplastic contamination in the bay of Marseille (French Mediterranean Sea) and its impact on zooplankton and mussels. Mar. Pollut. Bull. 175, 113353. https://doi.org/10.1016/j.marpolbul.2022.113353

Godø, O.R., Samuelsen, A., Macaulay, G.J., Patel, R., Hjøllo, S.S., Horne, J., Kaartvedt, S., Johannessen, J.A., 2012. Mesoscale Eddies Are Oases for Higher Trophic Marine Life. PLoS ONE 7, e30161. https://doi.org/10.1371/journal.pone.0030161

Gorsky, G., Ohman, M.D., Picheral, M., Gasparini, S., Stemmann, L., Romagnan, J.-B., Cawood, A., Pesant, S., Garcia-Comas, C., Prejger, F., 2010. Digital zooplankton image analysis using the ZooScan integrated system. J. Plankton Res. 32, 285–303. https://doi.org/10.1093/plankt/fbp124

Gove, J.M., Whitney, J.L., McManus, M.A., Lecky, J., Carvalho, F.C., Lynch, J.M., Li, J., Neubauer, P., Smith, K.A., Phipps, J.E., Kobayashi, D.R., Balagso, K.B., Contreras, E.A., Manuel, M.E., Merrifield, M.A., Polovina, J.J., Asner, G.P., Maynard, J.A., Williams, G.J., 2019. Prey-size plastics are invading larval fish nurseries. Proc. Natl. Acad. Sci. 116, 24143–24149. https://doi.org/10.1073/pnas.1907496116

Guillaumot, C., Artois, J., Saucède, T., Demoustier, L., Moreau, C., Eléaume, M., Agüera, A., Danis, B., 2019. Broad-scale species distribution models applied to data-poor areas. Prog. Oceanogr. 175, 198–207. https://doi.org/10.1016/j.pocean.2019.04.007

Guisan, A., Thuiller, W., 2005. Predicting species distribution: offering more than simple habitat models. Ecol. Lett. 8, 993–1009. https://doi.org/10.1111/j.1461-0248.2005.00792.x

Hernández-Carrasco, I., Orfila, A., Rossi, V., Garçon, V., 2018. Effect of small scale transport processes on phytoplankton distribution in coastal seas. Sci. Rep. 8, 8613. https://doi.org/10.1038/s41598-018-26857-9

Jâms, I.B., Windsor, F.M., Poudevigne-Durance, T., Ormerod, S.J., Durance, I., 2020.

797 Estimating the size distribution of plastics ingested by animals. Nat. Commun. 11,
798 1594. https://doi.org/10.1038/s41467-020-15406-6
799 Kershaw, P.J., Turra, A., Galgani, F., 2019. Guidelines for the monitoring and assessment of
800 plastic litter and microplastics in the ocean.
801 Lattin, G.L., Moore, C.J., Zellers, A.F., Moore, S.L., Weisberg, S.B., 2004. A comparison of
802 neustonic plastic and zooplankton at different depths near the southern California
803 shore. Mar. Pollut. Bull. 49, 291–294. https://doi.org/10.1016/j.marpolbul.2004.01.020
804 Lau, W.W.Y., Shiran, Y., Bailey, R.M., Cook, E., Stuchtey, M.R., Koskella, J., Velis, C.A.,
805 Godfrey, L., Boucher, J., Murphy, M.B., Thompson, R.C., Jankowska, E., Castillo
806 Castillo, A., Pilditch, T.D., Dixon, B., Koerselman, L., Kosior, E., Favoino, E.,
807 Gutberlet, J., Baulch, S., Atreya, M.E., Fischer, D., He, K.K., Petit, M.M., Sumaila,
808 U.R., Neil, E., Bernhofen, M.V., Lawrence, K., Palardy, J.E., 2020. Evaluating
809 scenarios toward zero plastic pollution. Science 369, 1455–1461.
810 https://doi.org/10.1126/science.aba9475
811 Le Bourg, B., Bănaru, D., Saraux, C., Nowaczyk, A., Le Luherne, E., Jadaud, A., Bigot, J.L.,
812 Richard, P., 2015. Trophic niche overlap of sprat and commercial small pelagic
813 teleosts in the Gulf of Lions (NW Mediterranean Sea). J. Sea Res. 103, 138–146.
814 https://doi.org/10.1016/j.seares.2015.06.011
815 Lefebvre, C., Saraux, C., Heitz, O., Nowaczyk, A., Bonnet, D., 2019. Microplastics FTIR
816 characterisation and distribution in the water column and digestive tracts of small
817 pelagic fish in the Gulf of Lions. Mar. Pollut. Bull. 142, 510–519.
818 https://doi.org/10.1016/j.marpolbul.2019.03.025
819 Liubartseva, S., Coppini, G., Lecci, R., 2019. Are Mediterranean Marine Protected Areas
820 sheltered from plastic pollution? Mar. Pollut. Bull. 140, 579–587.
821 https://doi.org/10.1016/j.marpolbul.2019.01.022
822 Liubartseva, S., Coppini, G., Lecci, R., Clementi, E., 2018. Tracking plastics in the
823 Mediterranean: 2D Lagrangian model. Mar. Pollut. Bull. 129, 151–162.
824 https://doi.org/10.1016/j.marpolbul.2018.02.019

825 Mansui, J., Darmon, G., Ballerini, T., van Canneyt, O., Ourmieres, Y., Miaud, C., 2020.
826 Predicting marine litter accumulation patterns in the Mediterranean basin: Spatio-
827 temporal variability and comparison with empirical data. Prog. Oceanogr. 182,
828 102268. https://doi.org/10.1016/j.pocean.2020.102268
829 Moore, C.J., Moore, S.L., Weisberg, S.B., Lattin, G.L., Zellers, A.F., 2002. A comparison of
830 neustonic plastic and zooplankton abundance in southern California's coastal waters.
831 Mar. Pollut. Bull. 44, 1035–1038. https://doi.org/10.1016/S0025-326X(02)00150-9
832 Morgado, C., Martins, A., Rosso, M., Moulins, A., Tepsich, P., 2017. Fin Whale Presence
833 and Distribution in the Pelagos Sanctuary: Temporal and Spatial Variability Along 2
834 Fixed-Line Transects Monitored in 2009-2013 14.
835 Moullec, F., Barrier, N., Drira, S., Guilhaumon, F., Hattab, T., Peck, M.A., Shin, Y.-J., 2022.
836 Using species distribution models only may underestimate climate change impacts
837 on future marine biodiversity. Ecol. Model. 464, 109826.
838 https://doi.org/10.1016/j.ecolmodel.2021.109826
839 Moullec, F., Barrier, N., Drira, S., Guilhaumon, F., Marsaleix, P., Somot, S., Ulses, C., Velez,
840 L., Shin, Y.-J., 2019a. An End-to-End Model Reveals Losers and Winners in a
841 Warming Mediterranean Sea. Front. Mar. Sci. 6, 345.
842 https://doi.org/10.3389/fmars.2019.00345
843 Moullec, F., Velez, L., Verley, P., Barrier, N., Ulses, C., Carbonara, P., Esteban, A., Follesa,
844 C., Gristina, M., Jadaud, A., Ligas, A., Díaz, E.L., Maiorano, P., Peristeraki, P.,
845 Spedicato, M.T., Thasitis, I., Valls, M., Guilhaumon, F., Shin, Y.-J., 2019b. Capturing
846 the big picture of Mediterranean marine biodiversity with an end-to-end model of
847 climate and fishing impacts. Prog. Oceanogr. 178, 102179.
848 https://doi.org/10.1016/j.pocean.2019.102179
849 Onink, V., Wichmann, D., Delandmeter, P., Sebille, E., 2019. The Role of Ekman Currents,
850 Geostrophy, and Stokes Drift in the Accumulation of Floating Microplastic. J.
851 Geophys. Res. Oceans 124, 1474–1490. https://doi.org/10.1029/2018JC014547
852 Pedrotti, M.L., Lombard, F., Baudena, A., Galgani, F., Elineau, A., Petit, S., Henry, M.,

Troublé, R., Reverdin, G., Ser-Giacomi, E., Kedzierski, M., Boss, E., Gorsky, G., 2022. An integrative assessment of the plastic debris load in the Mediterranean Sea. Sci. Total Environ. 838, 155958. https://doi.org/10.1016/j.scitotenv.2022.155958

Pedrotti, M.L., Petit, S., Elineau, A., Bruzaud, S., Crebassa, J.-C., Dumontet, B., Martí, E., Gorsky, G., Cózar, A., 2016. Changes in the Floating Plastic Pollution of the Mediterranean Sea in Relation to the Distance to Land. PLOS ONE 11, e0161581. https://doi.org/10.1371/journal.pone.0161581

Pennino, M.G., Bachiller, E., Lloret-Lloret, E., Albo-Puigserver, M., Esteban, A., Jadaud, A., Bellido, J.M., Coll, M., 2020. Ingestion of microplastics and occurrence of parasite association in Mediterranean anchovy and sardine. Mar. Pollut. Bull. 158, 111399. https://doi.org/10.1016/j.marpolbul.2020.111399

Picheral, M., Colin, S., Irisson, J.O., 2017. EcoTaxa, a tool for the taxonomic classification of images. URL Httpecotaxa Obs-Vlfr Fr.

Provencher, J.F., Ammendolia, J., Rochman, C.M., Mallory, M.L., 2019. Assessing plastic debris in aquatic food webs: what we know and don't know about uptake and trophic transfer. Environ. Rev. 27, 304–317. https://doi.org/10.1139/er-2018-0079

Queiros, Q., Fromentin, J.-M., Gasset, E., Dutto, G., Huiban, C., Metral, L., Leclerc, L., Schull, Q., McKenzie, D.J., Saraux, C., 2019. Food in the Sea: Size Also Matters for Pelagic Fish. Front. Mar. Sci. 6, 385. https://doi.org/10.3389/fmars.2019.00385

Ralston, D.K., Moore, S.K., 2020. Modeling harmful algal blooms in a changing climate. Harmful Algae 91, 101729. https://doi.org/10.1016/j.hal.2019.101729

Renzi, M., Specchiulli, A., Blašković, A., Manzo, C., Mancinelli, G., Cilenti, L., 2019. Marine litter in stomach content of small pelagic fishes from the Adriatic Sea: sardines (*Sardina pilchardus*) and anchovies (*Engraulis encrasicolus*). Environ. Sci. Pollut. Res. 26, 2771–2781. https://doi.org/10.1007/s11356-018-3762-8

Riandey, V., Champalbert, G., Carlotti, F., Taupier-Letage, I., Thibault-Botha, D., 2005. Zooplankton distribution related to the hydrodynamic features in the Algerian Basin (western Mediterranean Sea) in summer 1997. Deep Sea Res. Part Oceanogr. Res.

881 Pap. 52, 2029–2048. https://doi.org/10.1016/j.dsr.2005.06.004
882 Rochman, C.M., Tahir, A., Williams, S.L., Baxa, D.V., Lam, R., Miller, J.T., Teh, F.-C.,
883 Werorilangi, S., Teh, S.J., 2015. Anthropogenic debris in seafood: Plastic debris and
884 fibers from textiles in fish and bivalves sold for human consumption. Sci. Rep. 5,
885 14340. https://doi.org/10.1038/srep14340
886 Savoca, M.S., McInturf, A.G., Hazen, E.L., 2021. Plastic ingestion by marine fish is
887 widespread and increasing. Glob. Change Biol. 27, 2188–2199.
888 https://doi.org/10.1111/gcb.15533
889 Ser-Giacomi, E., Baudena, A., Rossi, V., Follows, M., Clayton, S., Vasile, R., López, C.,
890 Hernández-García, E., 2021. Lagrangian betweenness as a measure of bottlenecks
891 in dynamical systems with oceanographic examples. Nat. Commun. 12, 4935.
892 https://doi.org/10.1038/s41467-021-25155-9
893 Shin, Y.-J., Cury, P., 2001. Exploring fish community dynamics through size-dependent
894 trophic interactions using a spatialized individual-based model. Aquat Living Resour
895 16. https://doi.org/10.1016/S0990-7440(01)01106-8
896 Shin, Y.-J., Shannon, L.J., Cury, P.M., 2004. Simulations of fishing effects on the southern
897 Benguela fish community using an individual-based model: learning from a
898 comparison with ECOSIM. Afr. J. Mar. Sci. 26, 95–114.
899 https://doi.org/10.2989/18142320409504052
900 Simoncelli, S., Fratianni, C., Pinardi, N., Grandi, A., Drudi, M., Oddo, P., Dobricic, S., 2014.
901 Mediterranean Sea physical reanalysis (MEDREA 1987–2015)(Version 1). Copernic
902 Monit Env. Mar Serv CMEMS 10.
903 Siokou-Frangou, I., Christaki, U., Mazzocchi, M.G., Montresor, M., Ribera d'Alcalá, M.,
904 Vaqué, D., Zingone, A., 2010. Plankton in the open Mediterranean Sea: a review.
905 Biogeosciences 7, 1543–1586. https://doi.org/10.5194/bg-7-1543-2010
906 Solomando, A., Pujol, F., Sureda, A., Pinya, S., 2022. Ingestion and characterization of
907 plastic debris by loggerhead sea turtle, *Caretta caretta*, in the Balearic Islands. Sci.
908 Total Environ. 826, 154159. https://doi.org/10.1016/j.scitotenv.2022.154159

Soto-Navarro, J., Jordá, G., Compa, M., Alomar, C., Fossi, M.C., Deudero, S., 2021. Impact of the marine litter pollution on the Mediterranean biodiversity: A risk assessment study with focus on the marine protected areas. Mar. Pollut. Bull. 165, 112169. https://doi.org/10.1016/j.marpolbul.2021.112169

Wei, T., Simko, V., Levy, M., Xie, Y., Jin, Y., Zemla, J., 2017. Package 'corrplot.' Statistician 56, e24.

Yates, K.L., Bouchet, P.J., Caley, M.J., Mengersen, K., Randin, C.F., Parnell, S., Fielding, A.H., Bamford, A.J., Ban, S., Barbosa, A.M., Dormann, C.F., Elith, J., Embling, C.B., Ervin, G.N., Fisher, R., Gould, S., Graf, R.F., Gregr, E.J., Halpin, P.N., Heikkinen, R.K., Heinänen, S., Jones, A.R., Krishnakumar, P.K., Lauria, V., Lozano-Montes, H., Mannocci, L., Mellin, C., Mesgaran, M.B., Moreno-Amat, E., Mormede, S., Novaczek, E., Oppel, S., Ortuño Crespo, G., Peterson, A.T., Rapacciuolo, G., Roberts, J.J., Ross, R.E., Scales, K.L., Schoeman, D., Snelgrove, P., Sundblad, G., Thuiller, W., Torres, L.G., Verbruggen, H., Wang, L., Wenger, S., Whittingham, M.J., Zharikov, Y., Zurell, D., Sequeira, A.M.M., 2018. Outstanding Challenges in the Transferability of Ecological Models. Trends Ecol. Evol. 33, 790–802. https://doi.org/10.1016/j.tree.2018.08.001

Zurell, D., Franklin, J., König, C., Bouchet, P.J., Dormann, C.F., Elith, J., Fandos, G., Feng, X., Guillera-Arroita, G., Guisan, A., Lahoz-Monfort, J.J., Leitão, P.J., Park, D.S., Peterson, A.T., Rapacciuolo, G., Schmatz, D.R., Schröder, B., Serra-Diaz, J.M., Thuiller, W., Yates, K.L., Zimmermann, N.E., Merow, C., 2020. A standard protocol for reporting species distribution models. Ecography 43, 1261–1277. https://doi.org/10.1111/ecog.04960